Structural Basis of Extended Spectrum TEM -Lactamases CRYSTALLOGRAPHIC, KINETIC, AND MASS SPECTROMETRIC INVESTIGATIONS OF ENZYME MUTANTS*

Laurent Maveyraud, Isabelle Saves, Odile Burlet-Schiltz, Peter Swarén, Jean-Michel Masson, Myriam Delaire, Lionel Mourey, Jean-Claude Promé, Jean-Pierre Samama

THE JOURNAL OF BIOLOGICAL CHEMISTRY
Vol. 271, No. 18, Issue of May 3, pp. 10482–10489, 1996

Printed in U.S.A.

Structural Basis of Extended Spectrum TEM β-Lactamases

CRYSTALLOGRAPHIC, KINETIC, AND MASS SPECTROMETRIC INVESTIGATIONS OF ENZYME MUTANTS*

(Received for publication, July 31, 1995, and in revised form, January 16, 1996)

Laurent Maveyraud‡§, Isabelle Saves§¶, Odile Burlet-Schiltz§‖, Peter Swarén‡, Jean-Michel Masson¶, Myriam Delaire¶, Lionel Mourey‡, Jean-Claude Promé‖, and Jean-Pierre Samama‡**

From the ‡Groupe de Cristallographie Biologique, ¶Groupe d'Ingéniérie des Protéines, and ‖Groupe de Spectrométrie de Masse du Laboratoire de Pharmacologie et de Toxicologie Fondamentales, 205 route de Narbonne, 31 077 Toulouse Cedex, France

The E166Y and the E166Y/R164S TEM-1 β-lactamase mutant enzymes display extended spectrum substrate specificities. Electrospray mass spectrometry demonstrates that, with penicillin G as substrate, the rate-limiting step in catalysis is the hydrolysis of the E166Y acyl-enzyme complex. Comparison of the 1.8-Å resolution x-ray structures of the wild-type and of the E166Y mutant enzymes shows that the binding of cephalosporin substrates is improved, in the mutant enzyme, by the enlargement of the substrate binding site. This enlargement is due to the rigid body displacement of 60 residues driven by the movement of the Ω-loop. These structural observations strongly suggest that the link between the position of the Ω-loop and that of helix H5, plays a central role in the structural events leading to extended spectrum TEM-related enzymes. The increased Ω-loop flexibility caused by the R164S mutation, which is found in several natural mutant TEM enzymes, may lead to similar structural effects. Comparison of the kinetic data of the E166Y, E166Y/R164S, and R164S mutant enzymes supports this hypothesis.

Bacterial resistance to penicillins and cephalosporins represents an increasing risk in the chemotherapy of Gram-negative bacterial infections. This resistance often arises from the emergence and the dissemination of the plasmid-encoded extended spectrum β-lactamases (EC 3.5.2.6) (Blazquez *et al.*, 1995; Palzkill *et al.*, 1995; Venkatachalam *et al.*, 1994; Viadiu *et al.*, 1995). Most of these proteins are derived from the *Escherichia coli* TEM enzyme, via the combination of a few point mutations, which have led, so far, to 27 TEM-related enzymes (Morosini *et al.*, 1995). The parent TEM-1 is a very efficient enzyme and hydrolyzes penicillin substrates through an acylation and a deacylation step (Swarén *et al.*, 1995). Extended spectrum TEM-related enzymes hydrolyze third generation cephalosporin substrates. Based on the kinetic data, two common characteristics of these enzymes are (i) a severalfold reduction in the catalytic turnover toward penicillins, and (ii) an increase in the catalytic efficiency against cephalosporin substrates (Raquet *et al.*, 1994; Sowek *et al.*, 1991).

At the molecular level, it appears that high catalytic efficiencies against the third generation cephalosporin oxyimino-β-lactams, such as cefotaxime and ceftazidime, are primarily linked, in natural TEM mutants, to the mutation of Arg^{164} (Naumovski *et al.*, 1992) or to the mutation of Gly^{238} (Jacoby *et al.*, 1991). In the x-ray structure of the TEM-1 enzyme (Brookhaven DataBank entry 1BTL) (Jelsch *et al.*, 1993), Arg^{164} forms two salt bridge interactions. These are important for the conformation and the stability of the Ω-loop region (residues 161–180). Some residues from this loop define the active site topology, while others, such as Glu^{166}, are essential for catalysis. Site-directed mutagenesis studies demonstrated the requirement for an acidic side chain in position 166 (Delaire *et al.*, 1991) and the involvement of Glu^{166} in the deacylation reaction (Adachi *et al.*, 1991). Both the acid-base properties and the position of this proton acceptor group are reflected in the value of the deacylation rate constant (Swarén *et al.*, 1995).

Gly^{238} resides at the C-terminal edge of strand S3, which borders the substrate binding site cavity, and is in van der Waals contact with Asn^{170} main-chain atoms in the Ω-loop. Detailed kinetic and mass spectrometric investigations on the G238S mutant enzyme demonstrated a significant decrease of the deacylation rate constant, likely related to a perturbation of the deacylation machinery (Saves *et al.*, 1995a).

The E166Y mutant displays one of the characteristic features of extended spectrum enzymes: similar activities toward penicillin and cephalosporin substrates (Delaire *et al.*, 1991). The high resolution structure of this mutant shows unexpected structural differences compared with the wild-type enzyme. Comparison of the kinetic data of the E166Y, E166Y/R164S, and R164S (Sowek *et al.*, 1991; Raquet *et al.*, 1994) mutant enzymes suggests that these structural differences may play a key role in extending the substrate specificity of the TEM-related enzymes.

EXPERIMENTAL PROCEDURES

Protein Production—Site-directed mutagenesis, protein expression, and purification was performed as described (Saves *et al.*, 1995b). For site-directed mutagenesis, the following oligonucleotides were used: E166Y, 3′-CTA GCA ACC ATA GGC CTC GAC-5′; and E166Y-R164S, 3′-CAT TGA GCG GAA CTA TCA ACC ATG GGC CTC GAC TTA CTT-5′.

Determination of Kinetic Parameters of Substrate Hydrolysis and Determination of Acylation and Deacylation Rate Constants by Electrospray Mass Spectrometry (ESMS)[1]—The Michaelis-Menten kinetic parameters and the elementary rate constants by ESMS were determined as described previously (Saves *et al.*, 1995a, 1995b).

Crystal Preparation—A solution of the E166Y mutant enzyme (14.5 mg/ml) in 45 mM potassium phosphate buffer (pH 7.8), containing 7.5% (v/v) saturated ammonium sulfate solution, was equilibrated, at 6 °C, against 100 mM potassium phosphate buffer (pH 7.8), containing 42%

* This work was supported, in part, by the Institut National de la Santé et de la Recherche Médicale (Contract 930612) and by Association pour la Recherche contre le Cancer (Contract 6564). The costs of publication of this article were defrayed in part by the payment of page charges. This article must therefore be hereby marked "*advertisement*" in accordance with 18 U.S.C. Section 1734 solely to indicate this fact.

§ These authors contributed equally to this work.

** To whom correspondence should be addressed: Groupe de Cristallographie Biologique du LPTF, CEMES-CNRS, BP 4347, 29 rue Jeanne Marvig, 31 055 Toulouse Cedex, France. Tel.: 33 62 25 78 08; Fax: 33 62 25 79 60; E-mail: samama@ecstasy.cemes.fr.

[1] The abbreviation used is: ESMS, electrospray mass spectrometry.

TABLE I
Data statistics by resolution shells between 1.73 and 8.0 Å

	Resolution shell lower limit (Å)						
	1.73	1.83	1.97	2.17	2.49	3.13	global
Number of observations	3879	10,151	13,275	16,160	30,239	36,803	110,507
Number of independent reflections	1616	3267	3700	3783	3922	4391	20,679
Completeness	38.6	77.4	87.7	89.3	91.5	98.3	80.7
⟨I⟩	130	177	257	334	504	1338	525
⟨I/σI⟩	8.6	13.0	19.4	27.6	53.4	112.7	45.3
$R_{sym}\ \frac{\Sigma\lvert I-\langle I\rangle\rvert}{\Sigma\lvert I\rvert}$	0.106	0.091	0.076	0.063	0.051	0.037	0.045

(v/v) saturated ammonium sulfate solution and 4% (v/v) acetone. After equilibration, the supersaturated medium was seeded with a TEM-1 wild-type microcrystal, and the ammonium sulfate was slowly increased to 47%. At this stage, the acetone was removed by slow evaporation. This procedure was repeated three times using, at each step, a newly formed E166Y crystal for seeding. Typical crystal size was 300 × 300 × 600 μm^3. E166Y crystals are isomorphous to wild-type TEM-1 crystals (space group $P2_12_12_1$), with cell parameters a = 43.1 Å, b = 64.4 Å, and c = 91.2 Å, and diffract to 1.73-Å resolution.

X-ray Data Collection and Processing—Data were collected from a single crystal on a Siemens/Nicolet area detector, mounted on a four-circle goniostat. Cu-Kα x-rays were generated with a Rigaku rotating anode, operating at 40 kV and 80 mA. The crystal-to-detector distance was 12 cm, and the swing angle was 20°. The crystal was cooled at −4 °C during data collection. Data frames of 0.2° oscillation range with exposure time of 60 s were collected. Data were processed with the Xengen package (Howard *et al.*, 1987) (Table I).

Structure Refinement—All calculations concerning structure factors and electron density maps were done using the CCP4 programs package (Collaborative Computational Project, 1994). Electron density maps and protein structures were displayed on an Evans & Sutherland ESV3/30–33 graphic system, using FRODO (Jones, 1985). Initial model corrections were manually applied according to ($3F_o - 2F_c$) and ($F_o - F_c$) difference Fourier maps computed between 8.0- and 3.0-Å resolution, using calculated structure factors from the refined wild-type structure. The resolution was extended to 2.0 Å in four steps of both simulated annealing with the X-PLOR 2.1 package (Brünger, 1990) (from 3000 to 300 K in 2.7 ps, time step of 0.025 ps) and manual corrections. Individual temperature factors were kept to 10 $Å^2$ in the first two refinement steps and were individually refined at 2.3- and 2.0-Å resolution. Solvent molecules were included as neutral oxygen atoms when they appeared as an electron density peak four standard deviations above the mean value in a ($F_o - F_c$) difference Fourier map, and at a reasonable distance from polar atoms. A tetrahedral arrangement of four positive electron density peaks was interpreted as a sulfate ion, provided by the crystallization medium, which was also found in the wild-type enzyme structure (Jelsch *et al.*, 1993). Further refinement included cycles of energy minimization, individual temperature factor refinement, solvent occupancy refinement with PROLSQ (Hendrickson and Konnert, 1980), and model inspection in ($2F_o - F_c$) and ($F_o - F_c$) electron density maps. For the comparison of the E166Y mutant and the wild-type enzyme structures, the C-α positions of residues from strands S1 (residues 43–50), S2 (residues 56–60), and S5 (residues 259–266) of the main β-sheet were chosen to determine the superposition parameters. These strands are identical in both structures and are far from the mutation site. Rotation and translation parameters were then applied to all atoms of the E166Y mutant protein. The root mean square differences are 0.13 Å for main-chain atoms (when the 85–142 and 165–170 regions are excluded from the calculation) and 0.31 and 0.48 Å for the 85–142 and 165–170 main-chain atoms, respectively. Positional differences given in the text for whole side chains and residues are root mean square differences.

RESULTS

Structure of the E166Y Mutant—The final R-factor for all reflections between 8- and 1.8-Å resolution was 0.163. The refined structure contained 194 water molecules and one sulfate ion, and the root mean square atomic positional error was estimated to be 0.14 Å from a σ_a plot (Read, 1986). The deviations from ideal geometry at the end of the refinement are given in Table II. As in the wild-type protein structure, Met^{69} and Leu^{220} are the only residues found in high energy conformations on a Ramachandran plot.

TABLE II
Deviations from ideal geometry at the end of refinement (resolution is 1.8 Å, R-factor is 0.163)

	Root mean square deviation from ideal value
Bond distance (Å)	0.019
Angle distance (Å)	0.052
Planar 1–4 distance (Å)	0.100
Planar restraints (Å)	0.024
Chiral center restraints ($Å^3$)	0.140
Trans peptide torsion angle restraint ω (degrees)	11.3

The overall structure of the E166Y β-lactamase is very similar to the 1.8-Å wild-type enzyme structure (Jelsch *et al.*, 1993). However, the E166Y mutation leads to significant structural differences in two areas: the region 165–170 (WYPELN), which is part of the Ω-loop, and residues 85–142, which move as a rigid body. This region contains helices H3 (109–111), H4 (119–128), and H5 (132–142) and two coil regions (86–108 and 112–118). It is part of the helical domain (residues 62–212) of class A β-lactamases (secondary structure assignment from Jelsch *et al.* (1993)).

The WYPELN Region—The movement of residues 165–170 (Fig. 1*A*) is directly related to the point mutation at position 166 and is restricted to these residues by the salt bridges Arg^{164}–Glu^{171} and Arg^{164}–Asp^{179}. In order to accommodate the bulkier phenol group, 166 C-α moves by 0.7 Å from its position in the wild-type structure, away from the protein core. Tyr^{166} OH is now at hydrogen bond distance (2.9 Å) from Ser^{70} O-γ compared with the 4.2-Å distance between Glu^{166} Oϵ-1 and Ser^{70} O-γ in the wild-type enzyme. This movement drives the displacement of Trp^{165} C-α and Pro^{167} C-α, found at 0.3 and 1.0 Å, respectively, from their positions in TEM-1. Movement of the Trp^{165} main-chain atoms, without significant modifications of its (ϕ,ψ) angles, forces the rotation of the indol ring that occupies the same steric volume. The C-α atoms of Glu^{168} and Leu^{169} move 0.5 and 0.2 Å, respectively, from their positions in the wild-type structure, but their side-chain conformations are little affected. More important changes occur for Asn^{170}, whose C-α is displaced by 0.5 Å and its side chain by 1 Å. There is no hydrogen bond exchanged between this side-chain amide group and Tyr^{166} OH, in contrast to the important interaction, formed in the wild-type structure, with the Glu^{166} carboxylate group. These structural modifications induce minimal effects on the main-chain atoms of Ser^{70} and Lys^{73}, which are shifted by 0.15 Å. However, Ser^{70} O-γ and Lys^{73} N-ζ move by 0.3 and 0.7 Å, respectively, and the amino group is now at hydrogen bond distance to Tyr^{166} OH (3.0 Å) (Fig. 1*A*).

These structural modifications within the Ω-loop affect the solvatation and the hydrogen bond network within the substrate binding site. Four water molecules are lost, and two water molecules and the sulfate ion are shifted compared with the wild-type enzyme (Fig. 1*B*). The water molecule Wat297,

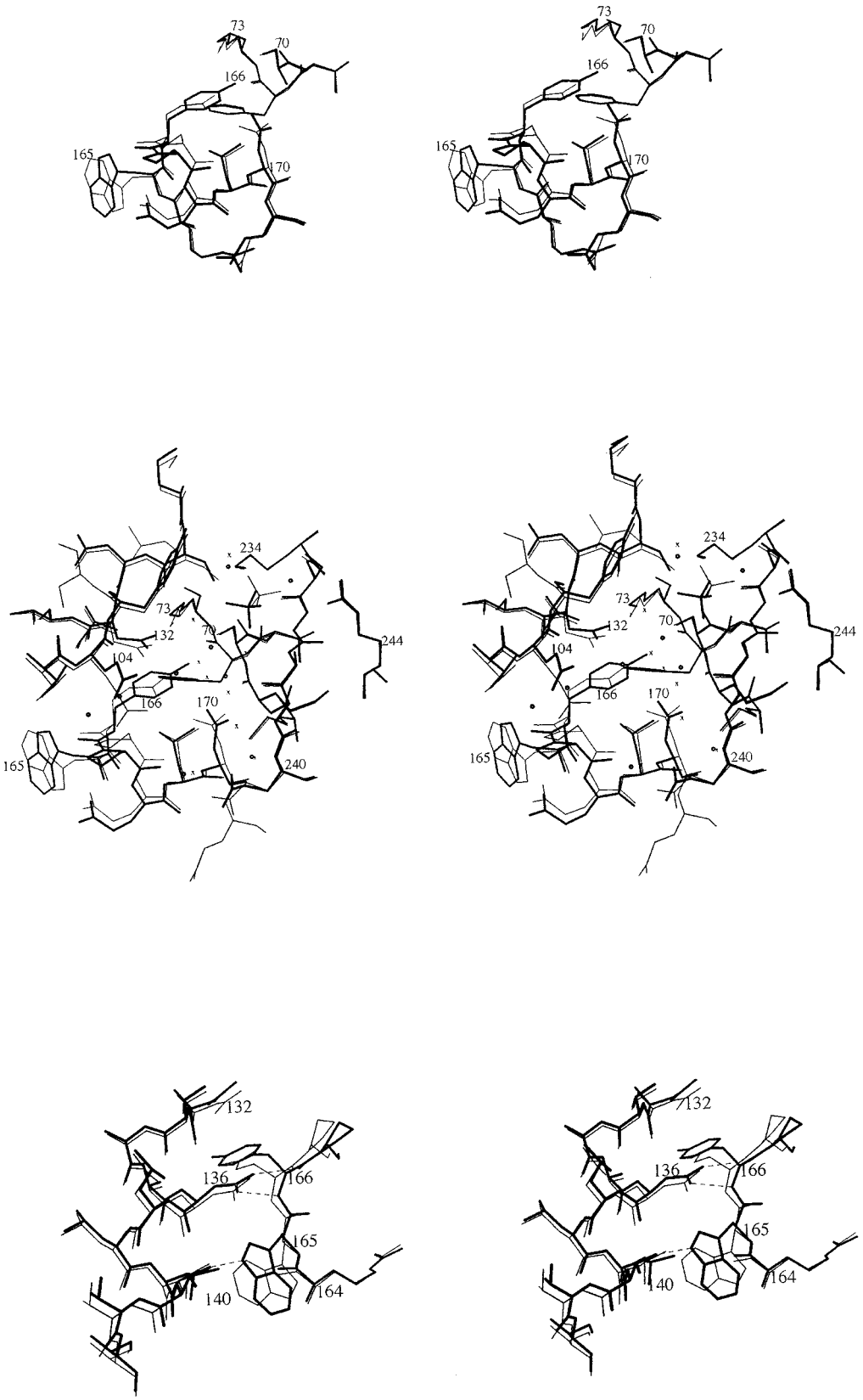

FIG. 1. *A*, stereo view of residues 70–73 and 165–170 in the wild-type (*thin lines*) and E166Y (*thick lines*) structures. *B*, stereo view of the substrate binding sites in the wild-type (*thin lines*) and E166Y (*thick lines*) structures. The crystallographic water molecules in the TEM-1 β-lactamase are represented by *crosses*. Those in the E166Y enzyme are represented by *dots*. The location of the sulfate ion is also represented. *C*, stereo view of the H5 helix (residues 132–142) and of residues 165–166 of the Ω-loop. The hydrogen bonds between the Asn^{136} side-chain atoms and the main-chain atoms of residue 166, and between Thr^{140} O-γ and Trp^{165} Nε are shown by *dotted lines*. The wild type is in *thin lines*, and the E166Y enzyme is in *thick lines*. The shifts in position for 166 C-α, 136 C-α and 140 O-γ are, respectively, of 0.7, 0.4, and 0.6 Å.

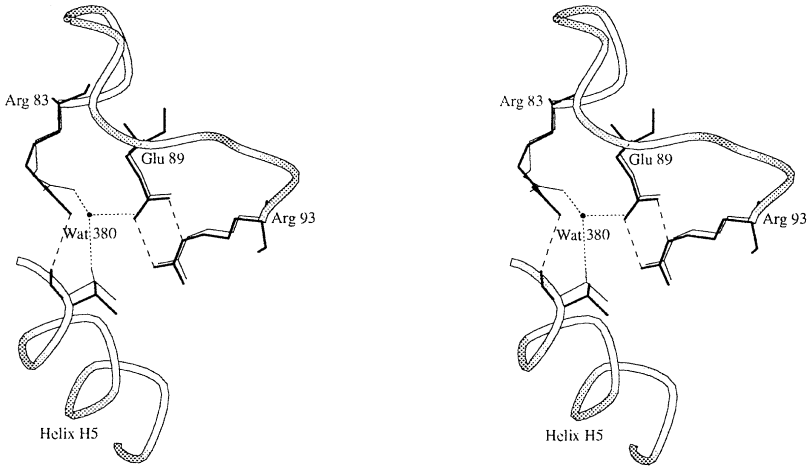

FIG. 2. **Stereo representation of the interactions in the wild-type enzyme (*thin* and *dotted lines*) and in the E166Y mutant enzyme (*thick* and *hatched lines*).** Arg^{83} and Thr^{141} are at the C termini of helices H2 and H5, respectively, and Glu^{89} and Arg^{93} are in the loop connecting H2 and H3. Wat380 in the wild-type enzyme is shown as a *dot*.

considered to be the nucleophile group in the deacylation step (Strynadka *et al.*, 1992; Jelsch *et al.*, 1993, Swarén *et al.*, 1995), is shifted by 1.5 Å but maintains hydrogen bonds to Ser^{70} nitrogen, Ser^{70} O-γ, Asn^{170} side-chain amide group, and Wat391. The 1-Å motion of the sulfate ion has several consequences: (i) it leads to the exclusion of Wat323 from the oxyanion hole, and of Wat404, found in the vicinity of Ser^{130} main-chain oxygen atom in the wild type structure, (ii) one of its oxygen atoms is now at hydrogen bond distance (2.9 Å) from Ala^{237} nitrogen, and (iii) it provides more space in the vicinity of the Ser^{130}, Ser^{235}, and Arg^{244} side chains in the E166Y structure, where a new water molecule (Wat518) is found. All other water molecules occupy nearly the same positions in both structures (Fig. 1*B*). Solvent molecules that are bound to residues of the Ω-loop move accordingly and preserve their interactions, except for the two water molecules (Wat422 and Wat472) that are expelled by the previously described Asn^{170} side-chain motion. However, the 1.0-Å displacement of Pro^{167} generates a cavity that is filled by a new water molecule.

The 85–142 Region—The rigid body motion of the region 85–142 is significant when comparing the wild-type and the E166Y structures, solved and refined at 1.8-Å resolution with *R*-factors of 0.160 and 0.163, respectively. Residues Asn^{132}, Asn^{136}, and Thr^{140}, located at three consecutive turns of helix H5, are in close contact with residues 165 and 166 and are directly affected by the Ω-loop movement (Fig. 1*C*). Asn^{132}, whose side chain is at van der Waals distance from the side chain of Glu^{166} in the wild-type structure, is displaced (main chain, 0.3 Å; side chain, 0.5 Å) as a result of the increased steric volume at position 166. Asn^{136}, located one helix turn away, whose amide side-chain atoms form two important hydrogen bonds to the Glu^{166} main-chain nitrogen and oxygen atoms in the wild-type structure, moves by 0.5 Å in order to preserve these interactions in the E166Y mutant. At the C terminus of helix H5, Thr^{140} O-γ moves by about 0.6 Å toward Trp^{165} N-ε, to which it is now hydrogen-bonded (Fig. 1*C*).

At the edges of this moving domain, residues Arg^{83} and Thr^{141}, at the C termini of helices H2 and H5, respectively, and Glu^{89} and Arg^{93}, in the connecting loop between helices H2 and H3, are clustered within a 4-Å radius sphere (Fig. 2). The movement of residue 141 induces the reorientation of the Arg^{83} side chain and the expulsion of Wat380, which was bridging Arg^{83} Nη-1, Glu^{89} Oε-1, and Thr^{141} O-γ in the wild-type structure. In the mutant enzyme, Arg^{83} Nη-1 is now hydrogen-bonded to the Thr^{141} main-chain oxygen atom.

Kinetics and Mass Spectrometry—Electrospray mass spectrometry experiments were used to determine the molecular weight of the E166Y mutant protein and of its molecular complexes. This soft ionization technique generates gas phase multicharged ions directly from the solution, and it allows characterization of the covalent intermediates of the reaction (Aplin *et al.*, 1990). The E166Y enzyme readily formed an acyl-enzyme intermediate with penicillin G. This complex (measured molecular mass of 29,318 ± 3 Da) was the only enzyme species that could be detected during the steady state of the reaction. Its formation was extremely fast, and no free mutant enzyme could be detected 10 s after the reaction was started, even at 2.5 °C. The difference between the molecular mass of this complex and that of the free mutant enzyme is in excellent agreement with the molecular mass of penicillin G (334 Da). The acyl-enzyme concentration was equal to the initial E166Y protein concentration, and the determined k_3 value at 37 °C (0.36 s^{-1}) is identical to the k_{cat} value measured from steady-state enzyme kinetics. In the mass range of the antibiotic, peaks corresponding to penicillin G and to the penicilloic acid reaction product (18 mass units higher) were followed during the time course of the reaction. After 5 min of reaction time at 37 °C, the only molecular species observed by ESMS were the acyl-enzyme complex (Fig. 3*A*), unreacted substrate, and the reaction product, penicilloic acid (Fig. 3*B*). When similar experiments were conducted with cephaloridin as substrate, we found that most of the enzyme was present in its free state (data not shown). The acyl-enzyme complex represented less than 10% of the total protein species. Its molecular mass indicated that the only reaction was the β-lactam cycle cleavage upon acyl-enzyme formation and that no elimination of the C-3′ substituent on the dihydrothiazine ring occurred. As previously discussed (Saves *et al.*, 1995a), a precise quantitation cannot be achieved on species amounting to 2–10% of the total ESMS signal.

The kinetic data of the E166Y and the E166Y/R164S mutant enzymes are reported in Table III. The single E166Y mutation led to improved K_m values for all substrates compared with the wild-type enzyme. However, compared with the E166Y enzyme, the E166Y/R164S double mutant enzyme discriminates between penicillin substrates (decreased K_m values) and cephalosporin substrates (increased K_m values). When compared with the wild-type enzyme, mutant proteins bearing the E166Y mutation display highly reduced k_{cat} values, although they are higher for cephalosporin than for penicillin substrates. These effects in K_m and k_{cat} led to modified substrate spectra in both mutant enzymes, a characteristic of extended spectrum TEM-related enzymes, as exemplified by the R164S TEM-1 mutant (Table III) (Sowek *et al.*, 1991; Raquet *et al.*, 1994). Taken together, these data suggest that the extended substrate spectra of these mutants arise from structural events common to all of these proteins.

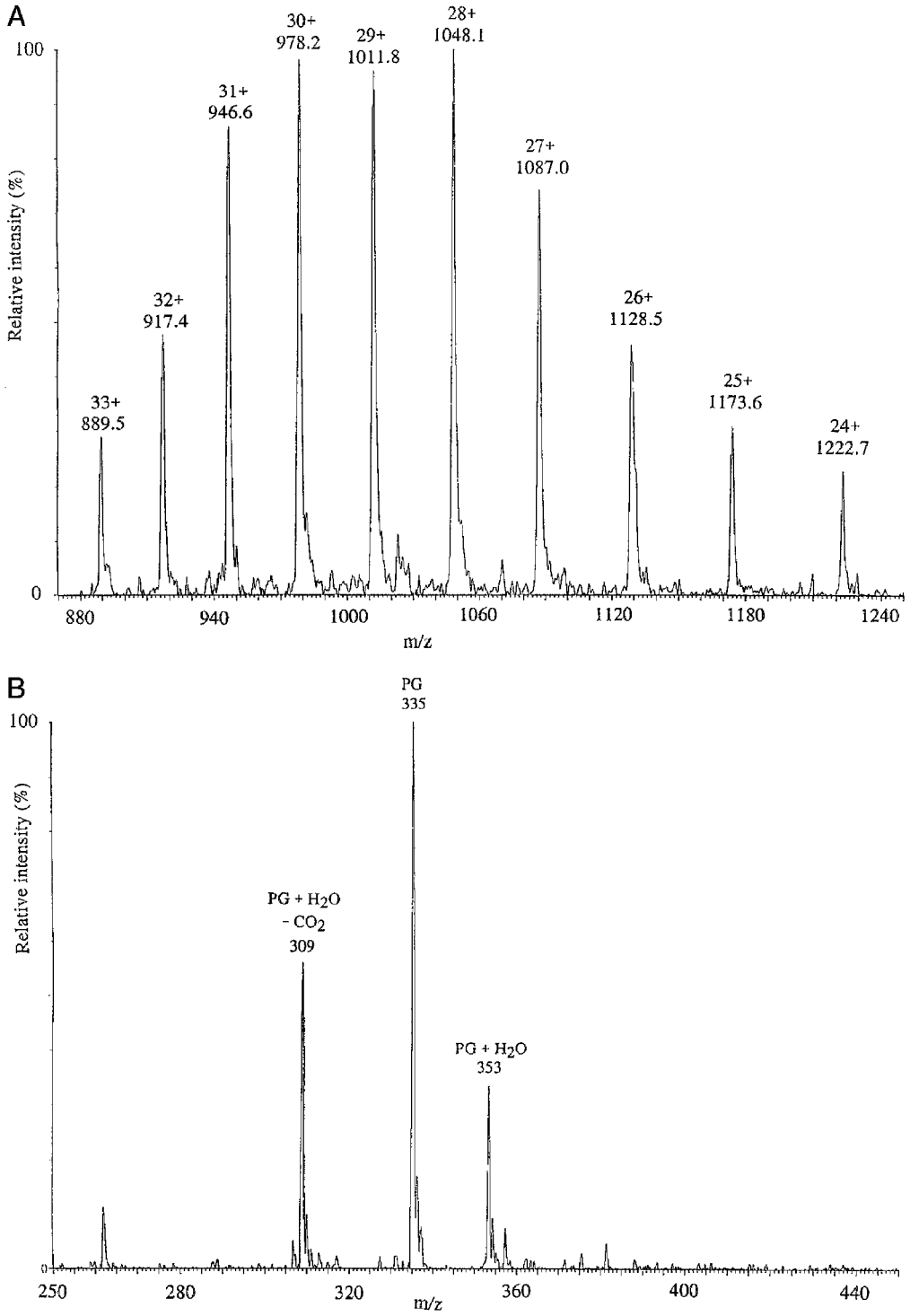

FIG. 3. *A*, electrospray mass spectra of the reaction mixture of E166Y and penicillin G at 37 °C after 5 min of reaction. The measured molecular mass from this peak distribution is 29,318 ± 3 Da, which corresponds to the covalent acyl-enzyme E166Y/penicillin G intermediate. *B*, singly charged ions are formed from low molecular mass molecules. Peaks labeled *PG* and *PG* + H_2O correspond to protonated penicillin G (substrate) and to protonated penicilloic acid (reaction product), respectively. The peak at *m*/*z* 309 corresponds to the decarboxylated (loss of 44 Da) penicilloic acid.

DISCUSSION

Effect of the E166Y Mutation on the Enzyme Structure and Consequences for the Binding of Cephalosporin Substrates—The structural modifications observed in the E166Y TEM-1 mutant are of two types. First, the mutation at position 166 induces the optimal short-range effect required to accommodate the larger side chain. Second, it induces an unexpected long range effect, in which a large part of the protein helical domain that bears important residues for catalysis is relocated.

The short range effect on the 165–170 Ω-loop region is restricted by the preceding Arg^{164} and the following Glu^{171}. Their side chains are engaged in two salt bridges that are important for the conformation and the stability of the Ω-loop and for the correct location of residue 166 within the active site. The salt bridge between Arg^{164} and Asp^{179} is buried and inaccessible to solvent molecules, which increases the strength of this interaction.

Three hydrogen bonds are exchanged between the Asn^{136}

TABLE III
Kinetic data of the TEM-1, E166Y, and E166Y/R164S enzymes

The data for the R164S mutant protein are from Raquet *et al.* (1994). Their data for TEM-1 are indicated by Footnote *b*. PG, penicillin G; AMX, amoxicillin; CD, cefaloridine; CFP, cefoperazone; CAZ, ceftazidime; CTX, cefotaxime; AZT, aztreonam; NCF, nitrocefine; ND, not determined.

Substrate	K_m		
	TEM-1	E166Y	E166Y/R164S
	μM	μM	μM
PG	60	12	4
AMX	40	33	20
CD	619	20	68
CFP	173	3	6
CAZ	1946	50	126
CTX	1100	—[a]	16
AZT	3888	237	541
NCF	20	13	31

Substrate	TEM-1		E166Y		E166Y/R164S		R164S	
	k_{cat}	PG	k_{cat}	PG	k_{cat}	PG	TEM-1	PG
	s^{-1}	%	s^{-1}	%	s^{-1}	%	%	%
PG	1243	100	0.36	100	0.71	100	2.5	100
AMX	1110	89	0.59	163	1.69	238	ND	
CD	1178	95	0.98	272	3.10	437	1.7	65
CTX	1.8	14	—[a]		0.53	75	16	3.8
CFP	513	41	0.95	263	1.75	246	ND	
NCF	418	34	0.24	67	0.48	67	4.6	107

Substrate	TEM-1		E166Y		E166Y/R164S		R164S	
	$k_{cat}k_m$	PG	k_{cat}/k_m	PG	k_{cat}/k_m	PG	TEM-1	PG
	$s^{-1}\ M^{-1}$	%	$s^{-1}\ M^{-1}$	%	$s^{-1}\ M^{-1}$	%	%	%
PG	2.1×10^7	100	3.0×10^4	100	1.8×10^5	100	15	100
AMX	2.8×10^7	133	1.8×10^4	60	8.5×10^4	47	ND	
CD	1.9×10^6	9	4.9×10^4	163	4.6×10^4	25	13	2.3
CFP	3.0×10^6	14	3.2×10^5	106	2.9×10^5	161	ND	
CAZ	—[a]	8.5×10^{-5}[b]	—[a]		—[a]		12,000	0.07
CTX	1.7×10^3	8×10^{-3}	—[a]		3.3×10^4	18	1000	0.1
AZT	—[a]	8×10^{-4}[b]	—[a]		—[a]		428	0.02
NCF	2.1×10^7	100	1.5×10^4	60	1.5×10^4	8	4	5

[a] Not measurable.
[b] Raquet *et al.* (1994) data for TEM-1.

side-chain and Glu^{166} main-chain atoms and between Thr^{140} O-γ and Trp^{165} N-ε. Thus, the movement of the 165–170 region leads to the concerted relocation of Asn^{132}, Asn^{136}, and Thr^{140} (Fig. 1*C*). This rigid body motion of the H5 helix drives the displacement of the whole 85–142 region, which represents one-third of the enzyme helical domain (Fig. 4). This movement requires only a few small main-chain dihedral angle rotations and preserves all of the interactions that occur within this protein domain.

The 85–142 region bears residues that delineate one side (residues 104–105, 130, 132) of the substrate binding cavity. The active site bottleneck is found between the hydroxyl groups of Ser^{130} and Ser^{235}, and is precisely the binding site of the thiazolidine ring of penicillins and of the dihydrothiazine ring of cephalosporins (Fig. 4). The distance between Ser^{130} O-γ and Ser^{235} O-γ is 5.4 Å in TEM-1 (Jelsch *et al.*, 1993). The movement of residues 85–142 in the E166Y enzyme increases this distance to 6.0 Å. As the K_I of cefotaxime, measured by competition procedures, is lowered 1500-fold compared with TEM-1 (Delaire *et al.*, 1991), we suggest that the increased active site aperture favors the better binding of cephalosporins. This is because the dihydrothiazine ring has a larger steric volume than the thiazolidine ring.

Mechanistic Aspects of the E166Y Mutation—Mass spectrometry measurements showed that during the steady state, the E166Y acyl-enzyme complex is the sole enzyme species with penicillin G as substrate. This indicates that the acylation rate is larger than the deacylation rate. Indeed, the determined k_3 value (0.36 s^{-1}) is 4000-fold smaller than the corresponding wild-type enzyme deacylation rate constant (1500 s^{-1}) (Christensen *et al.*, 1990). Since residue 166 is chemically involved in the deacylation step, a large decrease in k_3 could arise from the different acid-base properties of Tyr compared with Glu as a proton acceptor.

Within experimental errors, k_3 is identical to the k_{cat} value determined from steady-state kinetic measurements, which prevents calculation of k_2. However, examination of the k_{cat}/K_m values suggests slower acylation rates with the E166Y mutant enzymes compared with the wild-type enzyme. The role of Lys^{73} in the acylation reaction was recently described (Swarén *et al.*, 1995). Removal of the negative charge provided by Glu^{166} significantly decreases the basicity of the unprotonated Lys^{73} in the E166Y Michaelis complex, in line with the decrease of k_2 suggested by the steady-state kinetic data (detailed electrostatic calculations will be presented elsewhere).

ESMS experiments using cephaloridin showed that there is no elimination of the C-3′ substituent of the substrate forming the acyl-enzyme complex. Thus, the lower K_m values with the E166Y mutant protein for cephalosporin substrates do not arise from a change in the rate-limiting step resulting from a different kinetic pathway, as was shown to occur with the PC1 enzyme (Faraci and Pratt, 1985, 1986). The rate-limiting step for cephalosporin hydrolysis by the wild-type enzyme is acylation (Saves *et al.*, 1995a). A similar conclusion could be drawn for the E166Y mutant, as ESMS shows that more than 90% of the protein is found as free enzyme during the course of the reaction. However, the detection of a small amount of acyl-enzyme complex would suggest that the k_2 and k_3 values are of similar magnitude.

Kinetic Effects upon Mutation of Ω-Loop Residues—The crys-

FIG. 4. **Stereo view of the C-α chain tracing of the E166Y protein structure.** The regions that move relative to the wild-type enzyme are in *thick lines*. The bottleneck of the substrate binding site (between Ser^{130} O-γ and Ser^{235} O-γ) is indicated as well as penicillin G bound to the TEM-1 enzyme (from Swarén *et al.*, 1995).

tallographic refinement parameters indicate that the atomic positions in both structures have very little mobility, suggesting that both protein structures are representative of locked conformational states. In both enzymes, the Ω-loop conformation is severely constrained by the identical salt bridge interactions exchanged by Arg^{164}. The features of the x-ray structures provided the basis for comparing the kinetic data of the three mutant proteins: E166Y, E166Y/R164S, and R164S (Sowek *et al.*, 1991; Raquet *et al.*, 1994). They were examined with special emphasis on the Ω-loop conformation and flexibility, assigning a main role to residue 164.

In the TEM-1 enzyme, the R164*X* (except for lysine) mutation, by removing two out of the four salt bridges of the Ω-loop, will release some, but not all, of its conformational constraints. This will likely affect the relative positions of the partners involved in the deacylation step. A slight displacement of the Ω-loop residue Glu^{166} will decrease the deacylation rate of good TEM-1 substrates. Indeed, this rate is related both to the direction of the electrostatic potential gradient between the Glu^{166} carboxylate and the ester carbonyl carbon of the acyl-enzyme complex, and to its magnitude, which is very sensitive to atomic positional differences (Swarén *et al.*, 1995). The reduction in k_{cat} is of 10–50-fold in the TEM-related enzymes bearing the Arg^{164} mutation (R164S, R164H, R164S/E104K, and R164S/E240K) but is only marginally affected in the E104K and E240K single mutants (Sowek *et al.*, 1991, Raquet *et al.*, 1994, Petit *et al.*, 1995). This proposal is consistent with the situation observed in the PC1 β-lactamase, where a single salt bridge (Arg^{164}–Asp^{179}) stabilizes the Ω-loop conformation. The substantial disorder of the loop resulting from the D179N mutation (Herzberg *et al.*, 1991), led in that case to a 600-fold decrease in the k_{cat} value for penicillin G.

The movement of the 85–142 region, in the E166Y mutant enzyme structure, explains why binding is improved for cephalosporin substrates compared with the wild-type enzyme. A similar movement of the 85–142 region can be assumed to occur in the E166Y/R164S mutant protein. Interestingly, the additional R164S mutation in the E166Y enzyme has no effect with respect to the substrate spectrum (k_{cat}/K_m) for cephalosporin substrates, whereas the single R164S mutation in TEM-1 led to major kinetic differences. This paradox is explained if one assumes that the R164S mutation allows structural perturbations similar to those observed, and already achieved, in the E166Y protein. It explains why the additional R164S mutation in the E166Y enzyme is kinetically silent and offers a structural explanation of the consequences of the Arg^{164} mutation in the wild-type enzyme.

We propose that the conformational constraints of the Ω-loop, partly controlled by residue 164, and the position of the 85–142 region are interdependent in the TEM-1 enzyme. However, in the R164*X* TEM-1 enzymes, this structural link would only be kinetically discernible when large substituents on the substrate molecule reach the Ω-loop residues, as is the case with third generation cephalosporin substrates (Raquet *et al.*, 1994). The release of short contacts, achieved by the Ω-loop movement that drives the 85–142 region, accounts for the kinetic effects that are consistently found in extended spectrum TEM-related enzymes bearing the Arg^{164} mutation. First, the improvement of the binding of large cephalosporin substrates (*i.e.* ceftazidime) should increase the catalytic efficiencies for such molecules relative to penicillin substrates. k_{cat}/K_m are, indeed, 1–3 orders of magnitude larger in the R164S mutant than in the wild-type enzyme (Table III). Second, the large k_{cat}/K_m differences found in TEM-1 within the cephalosporin substrates should level out in the R164*X* mutant enzymes. Indeed, the k_{cat}/K_m of cefaloridin *versus* ceftazidime is decreased from 3×10^4 in the TEM-1 enzyme to 33 in the R164S mutant enzyme. This property is fulfilled in all TEM mutant proteins bearing the R164*X* mutation (Sowek *et al.*, 1991; Raquet *et al.*, 1994).

Mutations that occur in the vicinity of the Ω-loop residues, such as G238S, were shown to drastically reduce the deacylation rate constant (Saves *et al.*, 1995a). Natural mutants in this position also display extended substrate spectra, and work is in progress that will further illustrate the involvement of the Ω-loop region in the molecular evolution of the TEM-1 β-lactamase.

Acknowledgment—We are grateful to Martin Welch for a critical reading of the manuscript.

REFERENCES

Adachi, H., Ohta, T., and Matsuzawa, H. (1991) *J. Biol. Chem.* **266,** 3186–3191
Aplin, R. T., Baldwin, J. E., Schofield, C. J., and Waley, S. G. (1990) *FEBS Lett.* **277,** 212–214
Blazquez J., Morosini, M.-I., Negri, M.-C., Gonzalez-Leiza, M., and Baquero, F. (1995) *Antimicrob. Agents Chemother.* **39,** 145–149
Brünger, A. T. (1990) *X-PLOR Manual, version 2.1,* The Howard Hugues Medical

Institute and Departement of Molecular Biophysics and Biochemistry, Yale University, New Haven, CT
Christensen, H., Martin, M. T., and Waley, S. G. (1990) *Biochem. J.* **266,** 853–861
Collaborative Computational Project, Number 4 (1994) *Acta Cryst.* **D50,** 760–763
Delaire, M., Lenfant, F., Labia, R., and Masson, J-M. (1991) *Protein Eng.* **4,** 805–810
Faraci, W. S., and Pratt, R. F. (1985) *Biochemistry* **24,** 903–910
Faraci, W. S., and Pratt, R. F. (1986) *Biochemistry* **25,** 2934–2941
Hendrickson, W. A., and Konnert, J. H. (1980) in *Biomolecular Structure, Function, Conformation and Evolution*, Vol. 1 (Srinivasan, R. ed) pp. 43–57, Pergamon Press, Oxford
Herzberg, O., Kapadia, G., Blanco, B., Smith, T. S., and Coulson, A. (1991) *Biochemistry* **30,** 9503–9509
Howard, A. J., Gilliland, G. L., Finzel, B. C., Poulos, T. L., Ohlendorf, D. H., and Salemme, F. R. (1987) *J. Appl. Cryst.* **20,** 383–387
Jacoby, G. A., and Madeiros, A. A. (1991) *Antimicrob. Agents Chemother.* **35,** 1697–1704
Jelsch, C., Mourey, L., Masson, J.-M., and Samama, J-P. (1993) *Proteins Struct. Funct. Genet.* **16,** 364–383
Jones, T. A. (1985) *Methods Enzymol.* **115,** 157–171
Morosini, M. I., Canton, R., Martinez-Beltran, J., Negri, M. C., Perez-Diaz, J. C., Baquero, F., and Blazquez, J. (1995) *Antimicrob. Agents Chemother.* **39,** 458–461
Naumovski, L., Quinn, J. P., Miyashiro, D., Patel, M., Bush, K., Singer, S. B., Graves, D., Palzkill, T. and Arvin, A. M. (1992) *Antimicrob. Agents Chemother.* **36,** 1991–1996
Palzkill, T., Thomson, K. S., Sanders, C. C., Moland, E. S., Huang, W., and Milligan, T. W. (1995) *Antimicrob. Agents Chemother.* **39,** 1199–1200
Petit, A., Maveyraud, L., Lenfant, F., Samama, J-P., Labia, R., and Masson, J-M. (1995) *Biochem. J.* **305,** 33–40
Raquet, X., Lamotte-Brasseur, J., Fonzé, E., Goussard, S., Courvalin, P., and Frère, J-M. (1994) *J. Mol. Biol.* **244,** 625–639
Read, R. J. (1986) *Acta Cryst.* **A42,** 140–149
Saves, I., Burlet-Schiltz, O., Maveyraud, L., Samama, J-P., Promé, J-C., and Masson, J-M. (1995a) *Biochemistry* **34,** 11660–11667
Saves, I., Burlet-Schiltz, O., Swarén, P., Lefèvre, F., Masson, J.-M., Promé, J-C., and Samama, J-P. (1995b) *J. Biol. Chem.* **270,** 18240–18245
Sowek, J. A., Singer, S. B., Ohringer, S., Malley, M. F., Dougherty, T. J., Gougoutas, J. Z., and Bush, K. (1991) *Biochemistry* **30,** 3179–3188
Strynadka, N. C. J., Adachi, H., Jensen, S. E., John, K., Sielecki, A., Betzel, C., Sutoh, K., and James, M. N. G. (1992) *Nature* **359,** 700–705
Swarén, P., Maveyraud, L., Guillet, V., Masson, J-M., Mourey, L., and Samama, J-P. (1995) *Structure* **3,** 603–613
Venkatachalam, K. V., Huang, W., LaRocco, M., and Palzkill, T. (1994) *J. Biol. Chem.* **269,** 23444–23450
Viadiu, H., Osuna, J., Fink, A. L., and Soberon, X. (1995) *J. Biol. Chem.* **270,** 781–787

Structural Basis of Extended Spectrum TEM -Lactamases: CRYSTALLOGRAPHIC, KINETIC, AND MASS SPECTROMETRIC INVESTIGATIONS OF ENZYME MUTANTS

Laurent Maveyraud, Isabelle Saves, Odile Burlet-Schiltz, Peter Swarén, Jean-Michel Masson, Myriam Delaire, Lionel Mourey, Jean-Claude Promé and Jean-Pierre Samama

J. Biol. Chem. 1996, 271:10482-10489.
doi: 10.1074/jbc.271.18.10482